

Absorption cross section of regular black holes in scalar-tensor conformal gravity

Yang Li[†] and Yan-Gang Miao^{*}

School of Physics, Nankai University, Tianjin 300071, China

 (Received 22 August 2021; accepted 30 January 2022; published 17 February 2022)

In terms of the complex angular momentum method, we compute the absorption cross section by analyzing a massless test scalar field around conformally related black holes. First, we investigate circular null geodesics and thereby prove a precondition for calculating the absorption cross section in the context of conformally related black holes. Then we use the WKB approximation method to derive the analytic expression of Regge frequency and the oscillation part of absorption cross sections. We find that this oscillation part depends on the scale factor of conformal transformations. By taking the conformally related Schwarzschild-Tangherlini black hole as an example, we show that this regular black hole has substantially distinctive absorption behavior compared with singular black holes. Our result provides a new approach to distinguish a regular black hole from a singular one.

DOI: [10.1103/PhysRevD.105.044031](https://doi.org/10.1103/PhysRevD.105.044031)

I. INTRODUCTION

Searching for a gravitational theory beyond general relativity (GR) has never stopped since GR was realized to be imperfect as a theory of gravitation. A serious defect is that the black hole (BH) spacetimes in GR include singularities, which is not an honest reflection of astrophysical objects. Many gravitational theories have been proposed to solve this problem, among which the conformal gravity is a promising attempt [1–3]. Among various kinds of conformal gravitational theories that have been constructed so far, we focus on the conformal gravity from the scalar-tensor theory [4,5]. The reason is that some BH solutions of GR belong to the family of solutions of the scalar-tensor conformal gravitational theory. This is quite interesting. When a gravitational theory has a conformal invariance, one can obtain its metric by multiplying the metric of GR by a scale factor. As a consequence, the metric of the scalar-tensor conformal gravitational theory is composed of a GR metric multiplied by a scale factor. The black hole family obtained in this way is called conformally related black holes (CR BHs) and is usually a kind of regular black holes if a suitable scale factor is chosen.

The influence of scale factors is nontrivial. Significantly, the singularity located at the center of a BH can be removed [5,6] with a proper choice of scale factors, namely, CR BHs are usually regular. Besides the removing of spacetime singularities, various properties of CR BHs have been studied, including the quasinormal modes (QNMs) and

dynamic stability [6–8], thermodynamics and phase transitions [6,9,10], and the violation of energy conditions in CR BH spacetimes [11].

At present, the absorption property of CR BHs remains to be investigated. The absorption cross section (ACS) of a BH describes the interaction between the BH and the matter around it, which reflects the essential property of the BH. Some previous studies show [12–16] that the ACSs of regular BHs associated with nonlinear electrodynamics (NED) are not very different from those of the Reissner-Nordström BH. With fine tuning of parameters, the ACSs of the two kinds of BHs can even be the same. Because the Reissner-Nordström BH is singular, this phenomenon turns off the feasibility to distinguish the regular BHs associated with NED from singular ones by their ACSs. Nevertheless, the studies about the QNMs of CR BHs are inspiring, which indicates that this dynamic property is greatly distinct from that of singular BHs, depending on the choice of a scale factor. Therefore, it is of considerable value to investigate the ACSs of CR BHs from the perspective on distinguishing a regular BH from a singular one.

We adopt the complex angular momentum (CAM) method to derive the analytic expression of ACSs. The CAM method was originally applied to scattering problems in quantum mechanics. The pioneering progress was made by Watson [17], see the monographs by Newton [18] and Nussenzweig [19] for the details. The first application of the CAM method to a gravitational theory was accomplished by Chandrasekhar and Ferrari [20], followed by Andersson and Thylwe [21,22] who applied this technique to the Schwarzschild BH. Later, the connection between surface waves and QNMs was established [23] in terms of the CAM method, where the QNMs were regarded as the

^{*}Corresponding author.
miaoyg@nankai.edu.cn

[†]2120190123@mail.nankai.edu.cn

resonance modes of surface waves. Moreover, the related progress was made [24–29], which provided a general proposal to derive the analytic expression of Regge frequency and thereby to work out ACSs. Incidentally, one method rather than the CAM was once proposed [30] to calculate the Regge frequency. In this paper, we follow the way suggested in Refs. [23–29] but generalize it for dealing with CR BHs.

The outline of this paper is as follows. We briefly review the scalar-tensor conformal gravity in Sec. II A and then the BH scattering/absorption theory in Sec. II B. In Sec. III, we prove a precondition for calculating Regge frequency in the context of CR BHs. We derive in Sec. IV the analytic expression of Regge frequency by using the third-order WKB method and apply the formula to the models of conformally related Schwarzschild-Tangherlini black holes (CRST BHs). In Sec. V, we give the general expression of ACSs and show its dependence on scale factors. We illustrate our results by taking the models of CRST BHs as examples. Finally, we present our conclusions in Sec. VI.

II. GENERAL FORMALISM

A. Conformal gravity

The conformal gravitational theory we consider is described [4,5,7] by the action,

$$I_C = \frac{1}{2} \int d^D x \sqrt{-g} \phi \left(\frac{1}{4} \frac{D-2}{D-1} R \phi - \square \phi \right), \quad (1)$$

where ϕ is a massless scalar field, R the Ricci scalar, and $\square \equiv g^{\mu\nu} \nabla_\mu \nabla_\nu$ the covariant d'Alembertian. Equation (1) is invariant under the conformal transformations of $g_{\mu\nu}$ and ϕ as follows:

$$g_{\mu\nu} \rightarrow S(x) g_{\mu\nu}, \quad (2)$$

$$\phi \rightarrow [S(x)]^{(2-D)/4} \phi, \quad (3)$$

where $S(x)$ denotes the scale factor.

There are many solutions of action Eq. (1). In general, $g_{\mu\nu}$ and ϕ depend on time. Here we focus on static solutions. In particular, if we choose $\phi = 2\sqrt{\frac{D-1}{D-2}}$, the conformal gravity reduces to the Einstein gravity. Therefore, there is a family of solutions in conformal gravity Eq. (1). This family of solutions is conformally related to the specific solution in the Einstein gravity through the conformal transformations Eqs. (2) and (3). Based on the metric of a spherically symmetric BH in the Einstein gravity, one can write [4,5,7] the metric of the family of conformally related BHs,

$$ds^2 = S(r) \left[-f(r) dt^2 + \frac{1}{f(r)} dr^2 + r^2 d\Omega_{D-2} \right], \quad (4)$$

where $f(r)$ is the lapse function in the Einstein gravity. Equation (4) is asymptotically flat in the D -dimensional spacetime because both $S(r)$ and $f(r)$ equal one in the limit of $r \rightarrow \infty$. With special choices of the scale factor, the spacetime singularity of Eq. (4) can be removed, which can be verified [4,6,8] by finite curvature invariants and complete geodesics in the spacetime.

B. Review of scattering/absorption theory

To study the dynamics of spacetime [Eq. (4)], one can investigate the simplest case; the minimally coupled massless scalar field. The dynamics of this test scalar field is described by the Klein-Gordon equation,

$$\frac{1}{\sqrt{-g}} \partial_\mu \sqrt{-g} g^{\mu\nu} \partial_\nu \Phi = 0. \quad (5)$$

The decomposition of Φ in the background of Eq. (4) has been introduced [6],

$$\Phi = \sum_{\ell, m} \frac{1}{r^{(D-2)/2} [S(r)]^{(D-2)/4}} e^{-i\omega t} \psi_\ell(r) Y_{\ell m}(\theta_1, \dots, \theta_{D-2}), \quad (6)$$

where $Y_{\ell m}(\theta_1, \dots, \theta_{D-2})$ stands for the spherical harmonics of $D-2$ angular coordinates, $0 \leq (\theta_1, \theta_2, \dots, \theta_{D-3}) \leq \pi$, and $0 \leq \theta_{D-2} \leq 2\pi$. With the help of Eqs. (5) and (6), one can obtain the Schrödinger-like equation,

$$\partial_{r_*}^2 \psi_\ell + (\omega^2 - V_\ell) \psi_\ell = 0, \quad (7)$$

with the effective potential,

$$V_\ell = f(r) \left\{ \frac{\ell(\ell + D - 3)}{r^2} + \frac{(f(r)(r^{(D-2)/2} [S(r)]^{(D-2)/4})')'}{[S(r)]^{(D-2)/4} r^{(D-2)/2}} \right\}, \quad (8)$$

where the ‘‘tortoise’’ coordinate r_* is defined as $dr_* \equiv dr/f(r)$ and the prime means the derivative with respect to the radial coordinate. The scalar wave is purely ingoing at the event horizon and outgoing at the spatial infinity. Under these boundary conditions, the eigenvalues ω of the master equation [Eq. (7)] are discrete. Therefore, one obtains [31–34] eigenmodes, i.e., the QNMs as well as the complex quasinormal frequencies (QNFs), $\omega = \omega_{\ell n} - i\Gamma_{\ell n}$, where $\omega_{\ell n}$ represents the oscillation and $\Gamma_{\ell n}$ the inverse of a damping time scale.

The dynamics of the test scalar field can also be understood in the perspective of BH scattering. The boundary conditions can be written explicitly as follows:

- (a) At the event horizon, the partial wave $\psi_\ell(r)$ is purely ingoing without reflection,

$$\psi_\ell(r) \sim e^{-i\omega r_*}, \quad r_* \rightarrow -\infty; \quad (9)$$

- (b) At the spatial infinity, $\psi_\ell(r)$ is asymptotically free,

$$\begin{aligned} \psi_\ell(r) \sim & \frac{1}{T_\ell(\omega)} e^{-i\omega r_* + i(\ell + \frac{D-3}{2})\frac{\pi}{2} - i\frac{\pi}{4}} \\ & - \frac{S_\ell(\omega)}{T_\ell(\omega)} e^{+i\omega r_* - i(\ell + \frac{D-3}{2})\frac{\pi}{2} + i\frac{\pi}{4}}, \quad r_* \rightarrow +\infty. \end{aligned} \quad (10)$$

Note that $1/T_\ell(\omega)$ is the reflective coefficient, $S_\ell(\omega)$ is the element of diagonalized scattering matrix, and $S_\ell(\omega)/T_\ell(\omega)$ is the transmitted coefficient. The terms $\pm i(\ell + \frac{D-3}{2})\frac{\pi}{2} \mp i\frac{\pi}{4}$ on the exponentials are relative phase differences between the reflective and transmitted waves.

According to the boundary conditions, the scalar wave is asymptotically free at the spatial infinity, and thus it does not encounter any potential barriers. Therefore, the reflective coefficient in Eq. (10) should vanish, while the transmitted coefficient should survive. This implies that the boundary conditions pick the poles of the scattering matrix, at which both $T_\ell(\omega)$ and $S_\ell(\omega)$ are infinite, but the ratio $S_\ell(\omega)/T_\ell(\omega)$ is finite. As $S_\ell(\omega)$ is a function of both ℓ and ω , the poles can be interpreted in two perspectives.

In the first perspective, $S_\ell(\omega)$ is analytically continued to the complex ω -plane ($\omega \in \mathbb{C}$), while $\ell \in \mathbb{N}$ remains unchanged. In this case, the poles of the scattering matrix correspond to the QNFs. As a consequence, on the complex- ω plane, the scattering matrix $S_\ell(\omega)$ can be expanded in the vicinity of QNFs,

$$S_\ell(\omega) \propto \frac{\Gamma_{\ell n}}{2(\omega - \omega_{\ell n} + i\Gamma_{\ell n})}, \quad (11)$$

which is the Breit-Wigner type of resonances; see Appendix A of Ref. [25] for the details.

In the second perspective we adopt in this paper, $S_\ell(\omega)$ is analytically continued to the complex λ -plane (CAM plane) by defining $\lambda \equiv \ell + (D-3)/2$ first and then analytically continuing λ to be complex, while $\omega \in \mathbb{R}$ remains unchanged. In this case, the poles of the scattering matrix correspond to the Regge poles. Conventionally, the notation $\lambda_n(\omega)$, $n = 1, 2, \dots$, is used to distinguish different Regge poles.

As suggested in Refs. [23–29], one can interpret resonances as the surface waves traveling around a photon sphere and damping simultaneously. $\text{Re}\lambda_n(\omega)$ denotes the speed of circumnavigation of surface waves and $\text{Im}\lambda_n(\omega)$ the damping of surface waves. In fact, the QNFs are closely related to the Regge poles. When the resonances happen, i.e., the real part of Regge poles satisfies

$$\text{Re}\lambda_n(\omega_{\ell n}) = \ell + \frac{D-3}{2}, \quad \ell \in \mathbb{N}, \quad (12)$$

one can solve the real part of QNFs. In addition, the minus imaginary part of QNFs can be determined by the Regge poles,

$$\Gamma_{\ell n} = \frac{\text{Im}\lambda_n(\omega) \frac{d}{d\omega} \text{Re}\lambda_n(\omega)}{\left[\frac{d}{d\omega} \text{Re}\lambda_n(\omega) \right]^2 + \left[\frac{d}{d\omega} \text{Im}\lambda_n(\omega) \right]^2} \Big|_{\omega=\omega_{\ell n}}. \quad (13)$$

III. PROOF OF A PRECONDITION FOR CONFORMALLY RELATED BLACK HOLES

In this section, our main purpose is to prove a precondition used in the calculation of Regge frequency for CR BHs.

The location of a photon sphere of a static spherically symmetric BH is determined [35,36] by the following formulas for the trivial scale factor, $S(r) = 1$,

$$f'(r_c) - \frac{2}{r_c} f(r_c) = 0, \quad (14)$$

$$f''(r_c) - \frac{2}{r_c^2} f(r_c) < 0. \quad (15)$$

In fact, according to Ref. [25], one can approximatively obtain $r_0 \approx r_c$ in the large- ℓ limit, where r_0 stands for the peak of the effective potential V_ℓ [Eq. (8)]. We need this approximate result in CR BHs with the nontrivial $S(r)$. Our way to prove is straightforward: If r_c and r_0 are independent of $S(r)$ in the large- ℓ limit, the approximate result holds for CR BHs. This is what we call the precondition.

A. r_c independent of $S(r)$

We start with the line element Eq. (4) and restrict our discussion, without loss of generality, to the circular geodesic orbits within the equatorial plane. As shown by Chandrasekhar [35] and Cardoso [36], the Lagrangian of a particle moving along one of such orbits is¹

$$2\mathcal{L} = -S(r)f(r)\dot{t}^2 + \frac{S(r)}{f(r)}\dot{r}^2 + S(r)r^2\dot{\varphi}^2, \quad (16)$$

where the dot denotes the derivative with respect to the affine parameter τ , and φ stands for the azimuthal angular coordinate. The generalized momenta then take the forms,

$$p_t = -S(r)f(r)\dot{t} \equiv -E, \quad (17a)$$

$$p_\varphi = S(r)r^2\dot{\varphi} \equiv L, \quad (17b)$$

¹Due to the different sign conventions, Eq. (16) is different from the Lagrangian in Ref. [36] by a minus sign.

$$p_r = \frac{S(r)}{f(r)} \dot{r}, \quad (17c)$$

where E and L are conserved energy and angular momentum of the moving particle, respectively. Solving Eq. (17) for \dot{t} and $\dot{\phi}$, we obtain

$$\dot{t} = \frac{E}{S(r)f(r)}, \quad (18)$$

$$\dot{\phi} = \frac{L}{S(r)r^2}, \quad (19)$$

and thus give the conserved Hamiltonian,

$$\begin{aligned} 2\mathcal{H} &= 2(p_r \dot{t} + p_\phi \dot{\phi} + p_r \dot{r} - \mathcal{L}) \\ &= -S(r)f(r)\dot{t}^2 + \frac{S(r)}{f(r)}\dot{r}^2 + S(r)r^2\dot{\phi}^2 \\ &= -\frac{E^2}{S(r)f(r)} + \frac{S(r)}{f(r)}\dot{r}^2 + \frac{L^2}{S(r)r^2} \\ &\equiv \delta_1, \end{aligned} \quad (20)$$

where $\delta_1 = 0$ stands for null geodesics, while $\delta_1 = -1$ for timelike ones. Equation (20) can be recast into

$$\dot{r}^2 = V_r, \quad (21)$$

with

$$V_r = \frac{f(r)}{S(r)} \left[\delta_1 - \frac{L^2}{S(r)r^2} + \frac{E^2}{S(r)f(r)} \right], \quad (22)$$

where V_r denotes the geometric potential of particles. We note that V_r is different from the effective scattering potential V_ℓ .

The photon sphere consists of circular null geodesics at $r = r_c$, and these null geodesics are unstable orbits such that

$$V_r|_{r=r_c} = 0 = V'_r|_{r=r_c}, \quad (23)$$

and

$$V''_r|_{r=r_c} < 0. \quad (24)$$

Equation (23) determines the value of r_c , while Eq. (24) shows the instability of orbits. We can write Eq. (23) explicitly,

$$V_r|_{r=r_c} = 0 \Rightarrow \frac{E^2}{f_c} - \frac{L^2}{r_c^2} = 0, \quad (25)$$

and

$$V'_r|_{r=r_c} = 0 \Rightarrow \left(\frac{E^2}{[S(r)]^2} - \frac{L^2 f(r)}{r^2 S(r)} \right)' \Big|_{r=r_c} = 0, \quad (26)$$

where f_c means $f(r_c)$. The similar notation is also applied to the scale factor, i.e., $S_c \equiv S(r_c)$, $S'_c \equiv S'(r_c)$, etc., in the following contexts. Equation (26) yields

$$2S'_c r_c (f_c L^2 - E^2 r_c^2) - L^2 S_c (2f_c - r_c f'_c) = 0. \quad (27)$$

Note that none of r_c , S_c , S'_c , and L equal zero. Substituting Eq. (25) into Eq. (27), we exactly obtain Eq. (14) which is associated with the trivial scale factor, $S(r) = 1$. Hence, we prove that r_c is independent of $S(r)$. In general, it is reasonable that the scale factor does not alter the location of photon spheres, since the equation of motion of null geodesics is conformally invariant.

B. r_0 independent of $S(r)$

Now we analyze V_ℓ for $\ell \gg 1$. V_ℓ has the following behavior in large- ℓ regimes for the CR BHs described by Eq. (4),

$$V_\ell \sim \frac{\ell^2 f(r)}{r^2}, \quad \ell \gg 1, \quad (28)$$

which can simply be verified when $\ell \gg 1$ is applied to Eq. (8) and the terms proportional to ℓ^0 and ℓ^1 are omitted. Note that Eq. (28) is exactly same as Eq. (44) of Ref. [36]. Therefore, the peak r_0 of V_ℓ in large- ℓ regimes is also independent of $S(r)$.

As a summary of Sec. III, the approximate result, $r_0 \approx r_c$ for $\ell \gg 1$, still holds for CR BHs with the nontrivial $S(r)$ because both r_0 and r_c are not altered by $S(r)$ in the large- ℓ limit. Incidentally, this implies that the geometric ACS, which will be discussed in detail in Sec. V, is independent of $S(r)$.

IV. REGGE FREQUENCY OF CONFORMALLY RELATED STATIC SPHERICALLY SYMMETRIC BLACK HOLES: WKB METHOD

In this section we calculate the Regge frequencies for CR BHs in terms of the third-order WKB method, which is the basis for us to investigate ACSs in the next section.

A. Regge frequency: General expression

Now we derive the analytic expression of Regge frequency via the third-order WKB method. Originally, the WKB method was used to derive the eigenvalues of Schrödinger equation in quantum mechanics; see Ref. [37] for a pedagogical introduction. Then it was introduced into BH perturbation theory for the calculation of QNMs, because the master equations of perturbative fields have the Schrödinger-like form and the QNMs correspond to the eigenvalues of Schrödinger-like equations. The first-order WKB method was applied by Schutz and Will [38], the

third-order one by Iyer and Will [39], the sixth-order one by Konoplya [40], and the higher-order one by Konoplya *et al.* [41,42]. Recently, the WKB method has also been used to calculate the Regge frequency in BH perturbation theory; see Ref. [23–25] for the details.

Here we resort to the third-order WKB method. As pointed out in Ref. [25], although the higher-order WKB

method has higher precision, the complexity of calculations also grows greatly, which gives rise to a too complicated analytic expression. As a primary application to CR BHs, the third-order WKB is good enough, which can be seen in the following discussions.

We start with the third-order WKB equation [39] in which the QNFs satisfy

$$\omega^2 = [V_0(\lambda) + [-2V_0^{(2)}(\lambda)]^{1/2}\bar{\Lambda}(\lambda, n)] - i\alpha(n)[-2V_0^{(2)}(\lambda)]^{1/2}[1 + \bar{\Omega}(\lambda, n)], \quad (29)$$

where $\omega \in \mathbb{R}^+$, λ is Regge frequency, $\lambda \in \mathbb{C}$, n is overtone number, $n \in \mathbb{N}^+$, and $\alpha(n) \equiv n - 1/2$. In Eq. (29) the two factors, $\bar{\Lambda}$ and $\bar{\Omega}$ take the forms,

$$\bar{\Lambda}(\lambda, n) = \frac{1}{[-2V_0^{(2)}(\lambda)]^{1/2}} \left[\frac{1}{8} \frac{V_0^{(4)}(\lambda)}{V_0^{(2)}(\lambda)} \left(\frac{1}{4} + [\alpha(n)]^2 \right) - \frac{1}{288} \left(\frac{V_0^{(3)}(\lambda)}{V_0^{(2)}(\lambda)} \right)^2 (7 + 60[\alpha(n)]^2) \right], \quad (30)$$

and

$$\begin{aligned} \bar{\Omega}(\lambda, n) = & \frac{1}{[-2V_0^{(2)}(\lambda)]} \left[\frac{5}{6912} \left(\frac{V_0^{(3)}(\lambda)}{V_0^{(2)}(\lambda)} \right)^4 (77 + 188[\alpha(n)]^2) \right. \\ & - \frac{1}{384} \left(\frac{[V_0^{(3)}(\lambda)]^2 V_0^{(4)}(\lambda)}{[V_0^{(2)}(\lambda)]^3} \right) (51 + 100[\alpha(n)]^2) + \frac{1}{2304} \left(\frac{V_0^{(4)}(\lambda)}{V_0^{(2)}(\lambda)} \right)^2 (67 + 68[\alpha(n)]^2) \\ & \left. + \frac{1}{288} \left(\frac{V_0^{(3)}(\lambda) V_0^{(5)}(\lambda)}{[V_0^{(2)}(\lambda)]^2} \right) (19 + 28[\alpha(n)]^2) - \frac{1}{288} \left(\frac{V_0^{(6)}(\lambda)}{V_0^{(2)}(\lambda)} \right) (5 + 4[\alpha(n)]^2) \right]. \quad (31) \end{aligned}$$

Moreover, the notation $V_0^{(p)}(\lambda)$ stands for the derivatives of $V_{\lambda-\frac{D-3}{2}}(r)$ with respect to the tortoise coordinate at the peak of the potential,

$$V_0^{(p)}(\lambda) = \left. \frac{d^p}{dr_*^p} V_{\lambda-\frac{D-3}{2}}(r_*) \right|_{r_*=r_{*0}}, \quad (32)$$

where $V_{\lambda-\frac{D-3}{2}}(r)$ corresponds to $V_\ell(r)$ that is now regarded as a function of complex λ after the analytic continuation of ℓ . We shall solve Eq. (29) approximatively by assuming $|\lambda| \gg 1$ and $|\text{Re}\lambda| \gg |\text{Im}\lambda|$. Such an assumption is just the precondition $r_0 \approx r_c$ for $\ell \gg 1$ that we just proved in the above section. So we evaluate $V_0^{(p)}(\lambda)$ at r_c rather than at r_0 . As done in Ref. [25], we also adopt η_c in order to simplify the formulas of Regge frequency,

$$\eta_c \equiv \frac{1}{2} \sqrt{4f_c - 2r_c^2 f_c^{(2)}}. \quad (33)$$

Again taking Eqs. (8), (32), and (33) into consideration, we compute the coefficients in Eqs. (29), (30), and (31).

These coefficients are related to $V_0^{(p)}(\lambda)$ and put in Appendix A.

Now it is ready to solve Eq. (29). By using Eqs. (30)–(32) together with Appendix A, we derive the general formula of the Regge frequency of CR BHs,

$$\begin{aligned} \lambda_n(\omega) \approx & \left[\frac{r_c^2}{f_c} \omega^2 + a_n + 2\eta_c^2 [\alpha(n)]^2 \varepsilon_n(\omega) \right]^{1/2} \\ & + i\eta_c \alpha(n) [1 + \varepsilon_n(\omega)], \quad (34) \end{aligned}$$

where

$$\varepsilon_n(\omega) = \frac{b_n}{(r_c^2/f_c)\omega^2 + a_n + \eta_c^2 [\alpha(n)]^2}. \quad (35)$$

Note that the formula has a similar form to that in Ref. [25], but the coefficients a_n and b_n are different from those in Ref. [25]. The condition, $|\lambda| \gg 1$ and $|\text{Re}\lambda| \gg |\text{Im}\lambda|$, leads to $\omega \gg 1$. Thus we can further expand $\lambda_n(\omega)$ in series of ω ,

$$\begin{aligned} \lambda_n(\omega) = & \left[\frac{r_c}{\sqrt{f_c}} \omega + \frac{a_n}{(2r_c/\sqrt{f_c})\omega} \right] \\ & + i\eta_c \alpha(n) \left[1 + \frac{b_n}{(r_c^2/f_c)\omega^2} \right] + \mathcal{O}\left(\frac{1}{\omega^3}\right). \quad (36) \end{aligned}$$

Here a_n and b_n depend on S_c and its derivatives $S_c^{(p)}$, and they encode nontrivial corrections to the Regge frequency

via the scale factor. Such nontrivial corrections show the major difference between the conformally related BHs and nonconformal ones. The expressions of a_n and b_n are presented in Appendix B. According to Eq. (36), the influence of $S(r)$ is efficiently suppressed in large- ω regimes. As a consequence, in high-frequency regimes, $\lambda_n(\omega) \approx r_c/\sqrt{f_c}\omega + i\eta_c\alpha(n)$, i.e., the Regge frequency becomes independent of the scale factor, which is consistent with the result of nonconformal BHs.

B. Regge frequency: The conformally related Schwarzschild-Tangherlini black hole

As an application of the result obtained in the above subsection, we give the expression of Regge frequency for conformally related Schwarzschild-Tangherlini black holes (CRST BHs) in the D -dimensional spacetime.

When $S(r) = 1$, CRST BHs return to ST BHs. For the two types of BHs, the lapse function is of the following form,

$$f(r) = 1 - \left(\frac{r_h}{r}\right)^{D-3}, \quad (37)$$

with

$$r_h^{D-3} = \frac{16\pi M}{(D-2)\mathcal{A}_{D-2}}, \quad \mathcal{A}_{D-2} = \frac{2\pi^{(D-1)/2}}{\Gamma[(D-1)/2]}, \quad (38)$$

where M is the mass, r_h is the radius of event horizons, \mathcal{A}_{D-2} is the area of unit sphere S^{D-2} , and $\Gamma[x]$ is the Gamma function. Using Eqs. (14), (33), (37), and (38), we compute the parameters, r_c and η_c ,

$$r_c = r_h \left(\frac{D-1}{2}\right)^{1/(D-3)}, \quad (39a)$$

$$\eta_c = \sqrt{D-3}. \quad (39b)$$

For illustration, we derive the Regge frequencies for the CRST BHs in four-, five-, and six-dimensional spacetimes, respectively, by using Eq. (36) together with Appendix B.

(a) $D = 4$ For the four-dimensional spacetime, considering Eqs. (37), (39a), and (39b), we have

$$r_c = \frac{3}{2}r_h = 3M, \quad (40a)$$

$$\eta_c = 1, \quad (40b)$$

$$\frac{r_c}{\sqrt{f_c}} = 3\sqrt{3}M. \quad (40c)$$

Thus, we obtain the Regge frequency from Eq. (36) and Appendix B,

$$\lambda_n(\omega) = \left[3\sqrt{3}M\omega + \frac{\sqrt{3}a_n}{18M\omega}\right] + i\alpha(n) \left[1 + \frac{b_n}{27M^2\omega^2}\right] + \mathcal{O}\left(\frac{1}{\omega^3}\right), \quad (41)$$

with

$$a_n = -\frac{29}{216} + \frac{1}{4S_c^2} [3M^2(S_c^{(1)})^2 - 6M^2S_cS_c^{(2)} - 8MS_cS_c^{(1)}] + \frac{5[\alpha(n)]^2}{18}, \quad (42a)$$

$$b_n = -\frac{371}{15552} - \frac{1}{8S_c^4} \{S_c^3[9M^4S_c^{(4)} + 42M^3S_c^{(3)} + 28M^2S_c^{(2)} - 4MS_c^{(1)}] \\ - 3S_c^2[6M^4(S_c^{(2)})^2 + 9M^4S_c^{(1)}S_c^{(3)} + 32M^3S_c^{(1)}S_c^{(2)} + 8M^2(S_c^{(1)})^2] \\ - 27M^4(S_c^{(1)})^4 + 9M^2S_c(S_c^{(1)})^2[7M^2S_c^{(2)} + 6MS_c^{(1)}]\} - \frac{305[\alpha(n)]^2}{3888}. \quad (42b)$$

(b) $D = 5$ Similarly, for the five-dimensional spacetime, we have

$$r_c = \sqrt{2}r_h = 4\sqrt{\frac{M}{3\pi}}, \quad (43a)$$

$$\eta_c = \sqrt{2}, \quad (43b)$$

$$\frac{r_c}{\sqrt{f_c}} = 4\sqrt{\frac{2M}{3\pi}}. \quad (43c)$$

The corresponding Regge frequency reads

$$\lambda_n(\omega) = \left[\sqrt{2}r_c\omega + \frac{a_n}{2\sqrt{2}r_c\omega} \right] + i\sqrt{2}\alpha(n) \left[1 + \frac{b_n}{2r_c^2\omega^2} \right] + \mathcal{O}\left(\frac{1}{\omega^3}\right), \quad (44)$$

with

$$a_n = -\frac{5}{16} + \frac{1}{2\pi S_c^2} [M(S_c^{(1)})^2 - 4MS_c S_c^{(2)} - 5\sqrt{3}\pi\sqrt{M}S_c S_c^{(1)}] + \frac{3[\alpha(n)]^2}{4}, \quad (45a)$$

$$\begin{aligned} b_n = & -\frac{101}{512} - \frac{1}{24\pi^2 S_c^4} \{S_c^3 [16M^2 S_c^{(4)} + 60\sqrt{3}\pi M^{3/2} S_c^{(3)} + 84\pi M S_c^{(2)} - 21\sqrt{3}\pi^{3/2}\sqrt{M}S_c^{(1)}] \\ & - S_c^2 [40M^4 S_c^{(1)} S_c^{(3)} + 120\sqrt{3}\pi M^{3/2} S_c^{(1)} S_c^{(2)} + 24M^2 (S_c^{(2)})^2 + 75\pi M (S_c^{(1)})^2] \\ & - 24M^2 (S_c^{(1)})^4 + 12MS_c (S_c^{(1)})^2 [5\sqrt{3}\pi M S_c^{(1)} + 6MS_c^{(2)}]\} - \frac{31[\alpha(n)]^2}{128}. \end{aligned} \quad (45b)$$

(c) $D = 6$ As done in the above two cases, for the six-dimensional spacetime, we have

$$r_c = \left(\frac{5}{2}\right)^{1/3} r_h = \frac{\sqrt[3]{15M}}{2^{2/3}\sqrt[3]{\pi}}, \quad (46a)$$

$$\eta_c = \sqrt{3}, \quad (46b)$$

$$\frac{r_c}{\sqrt{f_c}} = \frac{5^{5/6}\sqrt[3]{M}}{2^{2/3}\sqrt[6]{3\pi^2}}, \quad (46c)$$

and write the corresponding Regge frequency,

$$\lambda_n(\omega) = \left[\sqrt{\frac{5}{3}}r_c\omega + \frac{a_n}{2\sqrt{5/3}r_c\omega} \right] + i\sqrt{3}\alpha(n) \left[1 + \frac{b_n}{(5/3)r_c^2\omega^2} \right] + \mathcal{O}\left(\frac{1}{\omega^3}\right), \quad (47)$$

with

$$a_n = -\frac{31}{60} - \frac{3}{20\pi^{2/3}S_c} [(30M)^{2/3}S_c^{(2)} + 12\sqrt[3]{30\pi M}S_c^{(1)}] + \frac{7[\alpha(n)]^2}{5}, \quad (48a)$$

$$\begin{aligned} b_n = & -\frac{409}{720} - \frac{3}{800\pi^{4/3}S_c^3} \{S_c^2 [15\sqrt[3]{30M}M^{4/3}S_c^{(4)} + 480\sqrt[3]{\pi M}S_c^{(3)} \\ & + 56(30\pi)^{2/3}M^{2/3}S_c^{(2)} - 192\sqrt[3]{30\pi}\sqrt{M}S_c^{(1)}] \\ & - S_c [15\sqrt[3]{30M}(S_c^{(2)})^2 + 30\sqrt[3]{30M}S_c^{(1)}S_c^{(3)} \\ & + 840\sqrt[3]{\pi}M^{2/3}S_c^{(1)}S_c^{(2)} + 56(30\pi)^{2/3}\sqrt[3]{M}(S_c^{(1)})^2] \\ & + 30M^{2/3}(S_c^{(1)})^2 [12\sqrt[3]{\pi}M^{1/3}S_c^{(1)} + \sqrt[3]{30M}M^{2/3}S_c^{(2)}]\} - \frac{91[\alpha(n)]^2}{180}. \end{aligned} \quad (48b)$$

From the above Regge frequencies of CRST BHs, we find that a_n and b_n depend on M , S_c , and $S_c^{(p)}$ in a subtle way. In the second terms of a_n and b_n , the combination of M , S_c and $S_c^{(p)}$ is balanced such that the dimensions of all subterms in these second terms offset precisely with one another, which makes a_n and b_n exactly dimensionless. The powers of M in a_n and b_n are not uniform in different dimensional spacetimes because the dimension of mass changes with spacetime dimensions as shown in Eq. (38).

V. ABSORPTION CROSS SECTION

Based on the Regge frequency performed above, we are now ready to compute the ACSs for CR BHs. This section is divided into two subsections, where one focuses on the analytic expression of ACSs and the other to the illustration of ACSs in the models of CRST BHs.

A. Analytic expression of absorption cross sections

As shown in Refs. [26,43], the ACS of a D -dimensional static spherically symmetric BH reads²

$$\sigma_{\text{abs}}(\omega) = \frac{\pi^{(D-2)/2}}{\Gamma[(D-2)/2]\omega^{D-2}} \sum_{\ell=0}^{+\infty} \frac{\Gamma[\ell + D - 4]}{\Gamma[\ell]} \times (2\ell + D - 3)\Gamma_{\ell}(\omega), \quad (49)$$

where $\Gamma_{\ell}(\omega)$ denotes the graybody factor.³ Further, based on a modified version of Sommerfeld-Watson transformation [18], σ_{abs} can be analytically continued [26] such that $\ell + (D-3)/2 \equiv \lambda \in \mathbb{C}$. After these performances, one can rewrite σ_{abs} which consists of three parts,

$$\begin{aligned} \sigma_{\text{abs}}(\omega) &= \frac{2\pi^{(D-2)/2}}{\Gamma[(D-2)/2]\omega^{D-2}} \int_0^{+\infty} \frac{\Gamma[\lambda + (D-3)/2]}{\Gamma[\lambda - (D-5)/2]} \lambda \Gamma_{\lambda - \frac{D-3}{2}}(\omega) d\lambda \\ &\quad - \frac{4\pi^{D/2}}{\Gamma[(D-2)/2]\omega^{D-2}} \text{Re} \left[\sum_{n=1}^{+\infty} \frac{\Gamma[\lambda_n(\omega) + (D-3)/2]}{\Gamma[\lambda_n(\omega) - (D-5)/2]} \frac{e^{i\pi[\lambda_n(\omega) - (D-3)/2]} \lambda_n(\omega) \gamma_n(\omega)}{\sin[\pi(\lambda_n(\omega) - (D-3)/2)]} \right] \\ &\quad + \frac{\pi^{(D-2)/2}}{\Gamma[(D-2)/2]\omega^{D-2}} \int_0^{+\infty} \left[i \frac{\Gamma[\lambda + (D-3)/2]}{\Gamma[\lambda - (D-5)/2]} \frac{e^{i\pi[\lambda - (D-3)/2]} \lambda \Gamma_{\lambda - \frac{D-3}{2}}(\omega)}{\sin[\pi(\lambda - (D-3)/2)]} \right. \\ &\quad \left. + i \frac{\Gamma[-\lambda + (D-3)/2]}{\Gamma[-\lambda - (D-5)/2]} \frac{e^{i\pi[\lambda + (D-3)/2]} \lambda \Gamma_{-\lambda - \frac{D-3}{2}}(\omega)}{\sin[\pi(\lambda + (D-3)/2)]} \right] d\lambda, \end{aligned} \quad (50)$$

where $\gamma_n(\omega)$ is the residue of graybody factors at the n th Regge pole,

$$\gamma_n(\omega) \equiv \text{Res}[\Gamma_{\lambda - \frac{D-3}{2}}(\omega)]_{\lambda=\lambda_n(\omega)}, \quad (51)$$

The three terms in Eq. (50) play different roles. Let us give a detailed explanation.

The first term corresponds to the geometric absorption cross section, σ_{geo} , which has the following form [26],

$$\sigma_{\text{geo}} = \frac{\pi^{(D-2)/2} b_c^{D-2}}{\Gamma[D/2]}, \quad (52)$$

where $b_c \equiv r_c/\sqrt{f_c}$ is independent of $S(r)$. As a result, σ_{geo} is independent of $S(r)$, which indicates that the first term of Eq. (50) is out of our central concern.

We shall see that the third term of Eq. (50) is also out of our central concern. The reason is as follows. The integration with respect to λ leads to an overall factor. By definition, the graybody factor is the modulus square of transmission coefficients, so it is not larger than 1, namely, $\Gamma_{\lambda - \frac{D-3}{2}}(\omega) \leq 1$. Therefore, we know that the overall factor has an upper bound, which can be obtained by setting $\Gamma_{\lambda - \frac{D-3}{2}}(\omega) = 1$ in the third term of Eq. (50),

$$\int_0^{+\infty} \left\{ i \frac{\Gamma[\lambda + \frac{D-3}{2}]}{\Gamma[\lambda - \frac{D-5}{2}]} \frac{e^{i\pi(\lambda - \frac{D-3}{2})} \lambda}{\sin[\pi(\lambda - \frac{D-3}{2})]} + i \frac{\Gamma[-\lambda + \frac{D-3}{2}]}{\Gamma[-\lambda - \frac{D-5}{2}]} \frac{e^{i\pi(\lambda + \frac{D-3}{2})} \lambda}{\sin[\pi(\lambda + \frac{D-3}{2})]} \right\} d\lambda. \quad (53)$$

²This formula is valid for any effective potentials that are the function of radial coordinate only, so it is also valid in the CR BHs with a nontrivial scale factor. See also Ref. [44].

³Note to distinguish this factor from the Gamma function, $\Gamma[x]$.

By means of numerical integration of Eq. (53), we find that the effect of the third term of Eq. (50) is quite small if compared to that of the second term. In fact, within the intermediate frequency region that we concern most, the third term just contributes a minor correction to the total ACS. This will be further illustrated intuitively in Sec. VB.

The second term of Eq. (50) represents the contribution from the Regge poles. It manifests the oscillation behavior of ACSs with respect to ω , therefore it does contain the characteristic information of CR BHs. For this reason, the second term is our concern.

Now let us introduce the method we shall use for calculation of the second term of Eq. (50). Gamma functions have the property,

$$\frac{\Gamma(z+a)}{\Gamma(z+b)} \sim \left(\frac{1}{z}\right)^{-a+b}, \quad \text{if } |z| \rightarrow +\infty \quad \text{and} \quad |\arg z| < \pi. \quad (54)$$

Moreover, the sine function can approximately be reduced to

$$\begin{aligned} & \sin(\pi[\lambda_n(\omega) - (D-3)/2]) \\ &= \frac{1}{2i} [e^{i\pi[\lambda_n(\omega) - (D-3)/2]} - e^{-i\pi[\lambda_n(\omega) - (D-3)/2]}] \\ &= \frac{1}{2i} [e^{\pi\text{Im}\lambda_n(\omega)} (e^{i\pi[\text{Re}\lambda_n(\omega) - (D-3)/2]} e^{-2\pi\text{Im}\lambda_n(\omega)} \\ & \quad - e^{-i\pi[\text{Re}\lambda_n(\omega) - (D-3)/2]})] \\ &\approx -\frac{1}{2i} [e^{\pi\text{Im}\lambda_n(\omega)} e^{-i\pi[\text{Re}\lambda_n(\omega) - (D-3)/2]}], \end{aligned} \quad (55)$$

where we have omitted the term, $e^{i\pi[\text{Re}\lambda_n(\omega) - (D-3)/2]} \times e^{-2\pi\text{Im}\lambda_n(\omega)}$, because it is greatly suppressed by the factor $e^{-2\pi\text{Im}\lambda_n(\omega)}$. It is obvious to see that the leading order of $e^{-2\pi\text{Im}\lambda_n(\omega)}$ approximately equals 0.043 when $D = 4$ and $n = 1$ and it is even smaller when $D > 4$ and $n > 1$. By using Eqs. (54) and (55), we obtain the second term of Eq. (50) approximately as follows:

$$\begin{aligned} \sigma_{\text{abs}}^{\text{RP}}(\omega) &\approx \frac{8\pi^{D/2}}{\Gamma[(D-2)/2]\omega^{D-2}} \text{Re} \left[\sum_{n=1}^{+\infty} i e^{2i\pi[\text{Re}\lambda_n(\omega) - (D-3)/2]} \right. \\ & \quad \left. \times e^{-2\pi\text{Im}\lambda_n(\omega)} [\lambda_n(\omega)]^{D-3} \gamma_n(\omega) \right]. \end{aligned} \quad (56)$$

The graybody factor can be written [26] as

$$\Gamma_{\lambda-\frac{D-3}{2}}(\omega) = \left[1 + \exp\left(-2\pi \frac{\omega^2 - V_0(\lambda)}{\sqrt{-2V_0^{(2)}(\lambda)}}\right) \right]^{-1}. \quad (57)$$

Substituting Eq. (57) into Eq. (51), we compute $\gamma_n(\omega)$. Further substituting $\gamma_n(\omega)$ into Eq. (56), we finally obtain the explicit form of $\sigma_{\text{abs}}^{\text{RP}}(\omega)$.

In the following we focus on the CRST BH. Although the derivations are straightforward, the residues of graybody factors in D -dimensional spacetimes are not listed here except for those in the four-, five-, and six-dimensional spacetimes as a sample for CRST BHs.

(a) $D = 4$

$$\begin{aligned} \gamma_n(\omega) &= -\frac{1}{2\pi} - i \frac{\alpha(n)}{6\sqrt{3}\pi M\omega} \\ & \quad + \frac{1}{23328\pi M^2 S_c^4 \omega^2} \{486M^3 S_c (S_c^{(1)})^2 [7MS_c^{(2)} + 6S_c^{(1)}] - 151S_c^4 - 1458M^4 (S_c^{(1)})^4 \\ & \quad - 162M^2 S_c^2 [6M^2 (S_c^{(2)})^2 + 9M^2 S_c^{(1)} S_c^{(3)} + 32MS_c^{(1)} S_c^{(2)} + 8(S_c^{(1)})^2] \\ & \quad + 54MS_c^3 [9M^3 S_c^{(4)} + 42M^2 S_c^{(3)} + 28MS_c^{(2)} - 4S_c^{(1)}] - 276[\alpha(n)]^2 S_c^4\} + \mathcal{O}\left(\frac{1}{\omega^3}\right). \end{aligned} \quad (58)$$

(b) $D = 5$

$$\begin{aligned} \gamma_n(\omega) &= -\frac{1}{\sqrt{2}\pi} - i \frac{\sqrt{3}\alpha(n)}{4\sqrt{2}\pi M\omega} + \frac{1}{2048\sqrt{2}\pi^2 MS_c^4 \omega^2} \{96M^{3/2} S_c (S_c^{(1)})^2 [5\sqrt{3}\pi S_c^{(1)} + 6\sqrt{M} S_c^{(2)}] \\ & \quad - 192M^2 (S_c^{(1)})^4 - 111\pi^2 S_c^4 - 8MS_c^2 [24M(S_c^{(2)})^2 + 40MS_c^{(1)} S_c^{(3)} + 120\sqrt{3}\pi\sqrt{M} S_c^{(1)} S_c^{(2)} + 75\pi(S_c^{(1)})^2] \\ & \quad + 8\sqrt{M} S_c^3 [16M^{3/2} S_c^{(4)} + 60M\sqrt{3}\pi S_c^{(3)} + 84\sqrt{M}\pi S_c^{(2)} - 21\sqrt{3}\pi^{3/2} S_c^{(1)}]\} \\ & \quad - \frac{33[\alpha(n)]^2}{256\sqrt{2}M\omega^2} + \mathcal{O}\left(\frac{1}{\omega^3}\right). \end{aligned} \quad (59)$$

(c) $D = 6$

$$\begin{aligned}
 \gamma_n(\omega) = & -\frac{\sqrt{3}}{2\pi} - i \frac{3\sqrt[6]{3}\alpha(n)}{\sqrt[3]{25^{5/6}\pi^{2/3}\sqrt{M}\omega}} + \frac{1}{20000\sqrt{3}\pi^{5/3}M^{2/3}S_c^3\omega^2} \{270M(S_c^{(1)})^2[12\sqrt[3]{30\pi}(S_c^{(1)}) + 30^{2/3}M^{1/3}S_c^{(2)}] \\
 & - 1468\sqrt[3]{30}\pi^{4/3}S_c^3 - 135M^{2/3}S_c[(30M)^{2/3}(S_c^{(2)})^2 + 2(30M)^{2/3}S_c^{(1)}S_c^{(3)}] \\
 & + 56\sqrt[3]{30\pi}M^{1/3}S_c^{(1)}S_c^{(2)} + 112\pi^{2/3}(S_c^{(1)})^2\} + 27\sqrt[3]{M}S_c^2[5(30^{2/3})MS_c^{(4)} \\
 & + 160\sqrt[3]{30\pi}M^{2/3}S_c^{(3)} + 560\pi^{2/3}M^{1/3}S_c^{(2)} - 64(30^{2/3})\pi S_c^{(1)}\} \\
 & - \frac{11(3^{5/6})\sqrt[3]{2}[\alpha(n)]^2}{25(5^{2/3})\sqrt[3]{\pi}M^{2/3}\omega^2} + \mathcal{O}\left(\frac{1}{\omega^3}\right). \tag{60}
 \end{aligned}$$

In the final part of this subsection, we derive the analytic expressions of $\sigma_{\text{abs}}^{\text{RP}}(\omega)$ for the CRST BHs. We omit all contributions from the Regge poles of higher excitations, i.e., those with $n > 1$. The reason is same as that explained above, that is, all these contributions are suppressed by the exponential function $e^{-2\pi\text{Im}\lambda_n(\omega)}$, where $\text{Im}\lambda_n(\omega) = \eta_c\alpha(n) + \mathcal{O}(1/\omega^2) = \eta_c(n-1/2) + \mathcal{O}(1/\omega^2)$; see Eq. (36). Here we list the results in the four-, five-, and six-dimensional spacetimes.

 (a) $D = 4$

$$\begin{aligned}
 \sigma_{\text{abs}}^{\text{RP}}(\omega) = & -8e^{-\pi} \left[\frac{3\sqrt{3}M\pi \sin(6\sqrt{3}\pi M\omega)}{2\omega} - \frac{\pi \cos(6\sqrt{3}\pi M\omega)}{2\omega^2} \right. \\
 & \left. - \frac{\pi \sin(6\sqrt{3}\pi M\omega)}{1296\sqrt{3}MS_c^2\omega^3} (162M^2S_cS_c^{(2)} - 81M^2(S_c^{(1)})^2 + 216MS_cS_c^{(1)} + 61S_c^2) \right] + \mathcal{O}\left(\frac{1}{\omega^4}\right). \tag{61}
 \end{aligned}$$

 (b) $D = 5$

$$\begin{aligned}
 \sigma_{\text{abs}}^{\text{RP}}(\omega) = & 8e^{-\sqrt{2}\pi} \left[\frac{32\sqrt{2}M \sin[(8\sqrt{2}\pi M/3)\omega]}{3\pi^2\omega} - \frac{4\sqrt{6}M \cos[(8\sqrt{2}\pi M/3)\omega]}{\pi^{3/2}\omega^2} \right. \\
 & \left. - \frac{\sin[(8\sqrt{2}\pi M/3)\omega]}{4\sqrt{2}\pi^2S_c^2\omega^3} (16MS_cS_c^{(2)} - 4M(S_c^{(1)})^2 + 20\sqrt{3\pi}MS_cS_c^{(1)} + 13\pi S_c^2) \right] + \mathcal{O}\left(\frac{1}{\omega^4}\right). \tag{62}
 \end{aligned}$$

 (c) $D = 6$

$$\begin{aligned}
 \sigma_{\text{abs}}^{\text{RP}}(\omega) = & -8e^{-\sqrt{3}\pi} \left[\frac{25\sqrt{5}M \sin[(5^{5/6}\pi^{2/3}\sqrt[3]{2M}/\sqrt[6]{3})\omega]}{8\pi^2\omega} - \frac{5(15^{2/3})M^{2/3} \cos[(5^{5/6}\pi^{2/3}\sqrt[3]{2M}/\sqrt[6]{3})\omega]}{2\sqrt[3]{2}\pi^{5/3}\omega^2} \right. \\
 & \left. - \frac{\sqrt[3]{3}M \sin[(5^{5/6}\pi^{2/3}\sqrt[3]{2M}/\sqrt[6]{3})\omega]}{16\sqrt[6]{5}\pi^2S_c\omega^3} (9(15M)^{2/3}S_c^{(2)} + 54\sqrt[3]{60\pi}MS_c^{(1)} + 95\sqrt[3]{2}\pi^{2/3}S_c) \right] + \mathcal{O}\left(\frac{1}{\omega^4}\right). \tag{63}
 \end{aligned}$$

B. Graphs of $\sigma_{\text{abs}}^{\text{RP}}(\omega)$ for CRST BHs

Now we present the above results more intuitively in graphs. We restrict our attention onto the (CR)ST BHs and plot the behavior of $\sigma_{\text{abs}}^{\text{RP}}(\omega)$ with respect to ω . The dimensionless quantities, $\sigma_{\text{abs}}^{\text{RP}}(\omega)/A_h$ and $r_h\omega$, are adopted, where $A_h \equiv \mathcal{A}_{D-2}r_h^{D-2}$ is the area of event horizon of a $(D-2)$ -dimensional sphere. For simplicity, we refer to $\sigma_{\text{abs}}^{\text{RP}}(\omega)$ as the ‘‘oscillation’’ in the context.

First, in order to justify the correctness of our results, we show that our results are consistent with the Sinc results obtained in Ref. [26], where the latter is based on the model

of nonconformal Schwarzschild-Tangherlini BHs. Thus we set $S(r) = 1$ and choose the lapse function to be that of the Schwarzschild-Tangherlini BH in our results. We plot the comparison in Fig. 1, where the red and green curves agree with each other over a wide range. Only when the frequency is extremely low, does the disagreement appear slightly. The reason is that our results include $\mathcal{O}(1/\omega^3)$ corrections to $\sigma_{\text{abs}}^{\text{RP}}(\omega)$, while the Sinc results only include the order of $\mathcal{O}(1/\omega)$. Figure 1 manifests the consistency of our results with the Sinc’s. Moreover, this figure also justifies that the third term of Eq. (50) indeed contributes a minor correction to the total ACS; see the blue curves.

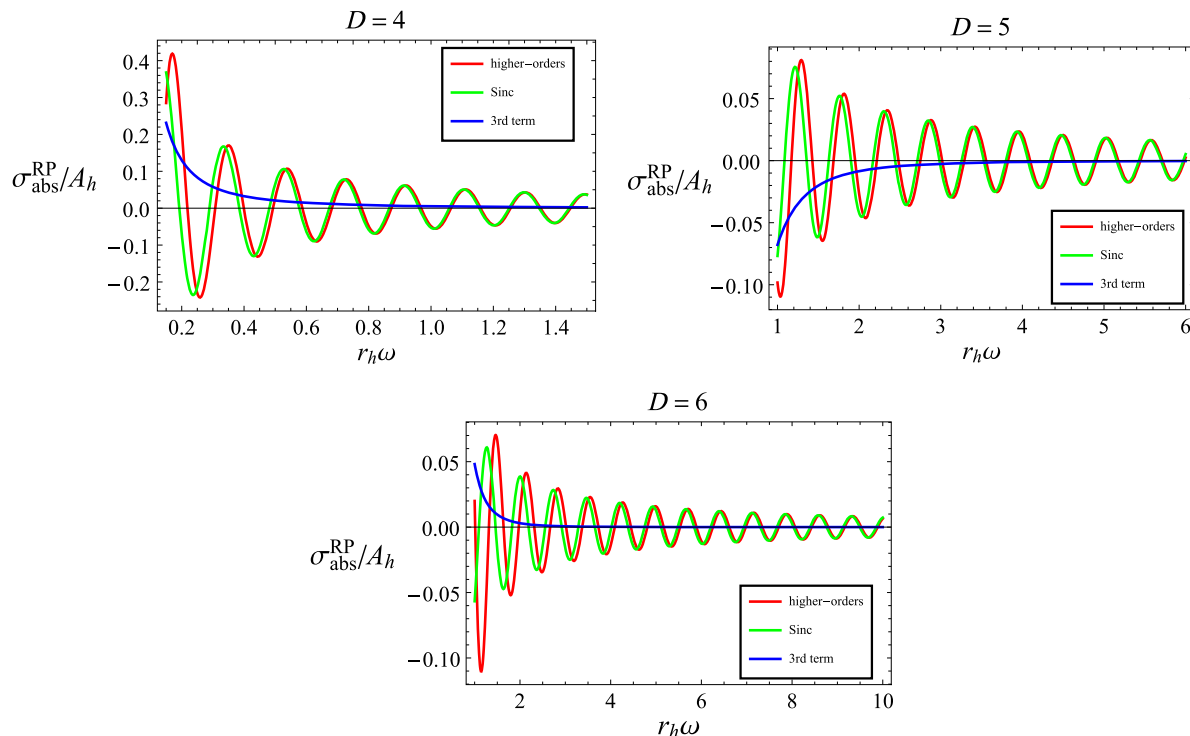


FIG. 1. The red curves stand for our results, the green curves for the Sinc ones in Ref. [26], and the blue curves for the upper bound of the third term in Eq. (50).

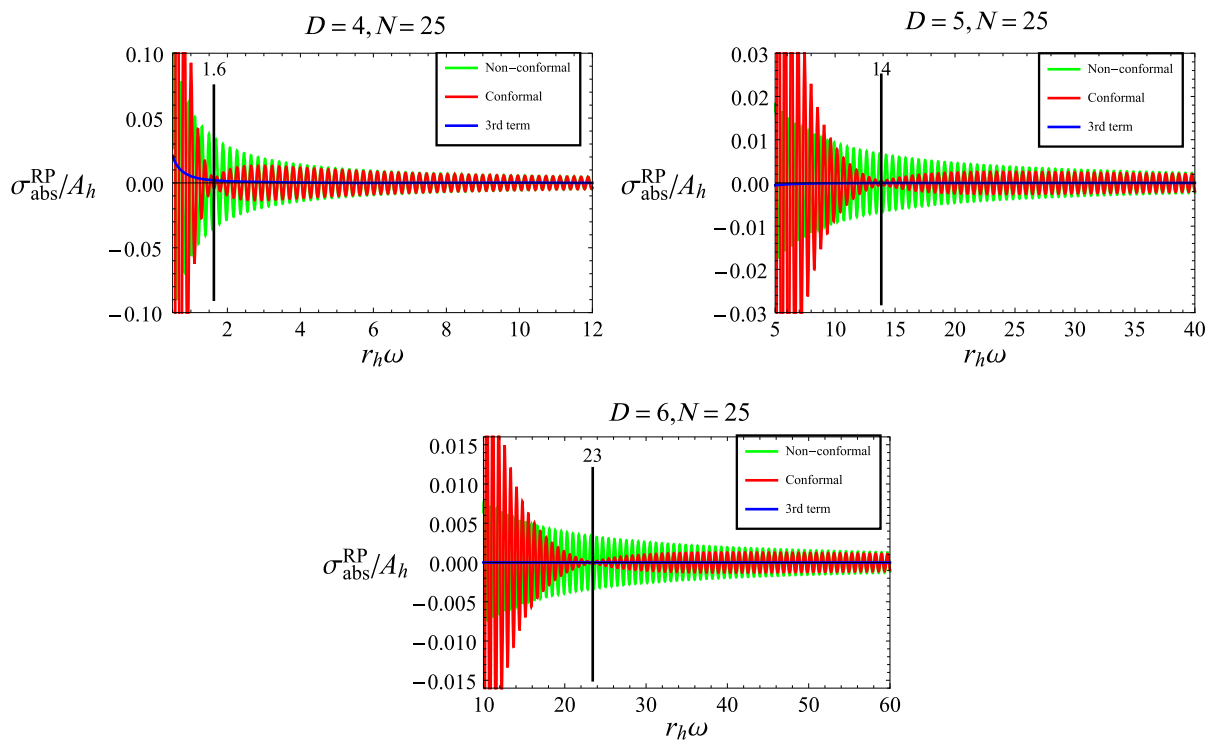


FIG. 2. Comparison between CRST BHs and ST BHs, where $L = r_c$ and $N = 25$ are chosen for the convenience of plotting. The red curves stand for the CRST BHs and the green curves for the ST BHs, where the vertical black lines mark the positions of “the minimum amplitude” in the four-, five-, and six-dimensional spacetimes, respectively. The blue curves stand for the upper bound of the third term in Eq. (50). Note that the blue curves are very close to the horizontal axes.

The effect of blue curves decreases rapidly when the frequency increases, such that it can be omitted in the intermediate region of frequency.

Next, we investigate the influence of scale factor $S(r)$ on $\sigma_{\text{abs}}^{\text{RP}}(\omega)$. This will be accomplished by studying the distinction between CRST BHs and ST BHs. We consider one specific kind of scale factors,

$$S(r) = 1 + \left(\frac{L}{r}\right)^{2N}, \quad (64)$$

where N is a dimensionless constant and L is a typical length scale of CRST BHs, e.g., r_h , or r_c , or the Planck length [4]. As long as N is large enough, the CRST BHs are free of spacetime singularity. In fact, we can verify that the Ricci scalar behaves as r^{2N-D+1} and the Kretschmann scalar as $r^{4N-2D+2}$ when $r \rightarrow 0$ for the choice of Eq. (64). If we take $N = 25$ in the four-, five-, and six-dimensional spacetimes in Fig. 2 and $N = 10, 25, 50, 100$ in the four-dimensional spacetime in Fig. 3, the corresponding CRST BHs are regular.

We present the behavior of $\sigma_{\text{abs}}^{\text{RP}}(\omega)$ with respect to ω in Fig. 2 by using Eqs. (61), (62), and (63), where the case of CRST BHs with nontrivial scale factors and the case of ST

BHs with the trivial scale factor ($N = 0$) are plotted. It is quite interesting that the amplitude of $\sigma_{\text{abs}}^{\text{RP}}(\omega)$ of CRST BHs always possesses a nonmonotonic behavior, unlike that of ST BHs which is monotonic. To show this phenomenon more clearly without loss of generality, we have made an appropriate choice of parameters, such as $N = 25$ and $L = r_c$. For the CRST BHs, the amplitude of $\sigma_{\text{abs}}^{\text{RP}}(\omega)$ is quite large in extremely low frequency regimes. As ω increases, the amplitude of $\sigma_{\text{abs}}^{\text{RP}}(\omega)$ decreases almost to zero at a certain value of ω which is called “the minimum amplitude”, and then the amplitude increases. Comparatively speaking, the amplitude of $\sigma_{\text{abs}}^{\text{RP}}(\omega)$ for the ST BHs decreases monotonically. In large- ω regimes, the oscillations of the two kinds of BHs go to the same value. We note that the effect of the third term of Eq. (50) can also be neglected; see the blue curves.

We further investigate the nonmonotonic behavior and find that it exists universally for a wide range of parameter N . To show this universality, we plot the results with various values of N for the four-dimensional CRST BH in Fig. 3. The situations for five- and six-dimensional models are similar and thus not presented here. We note that the effect of the third term of Eq. (50) can be neglected as expected.

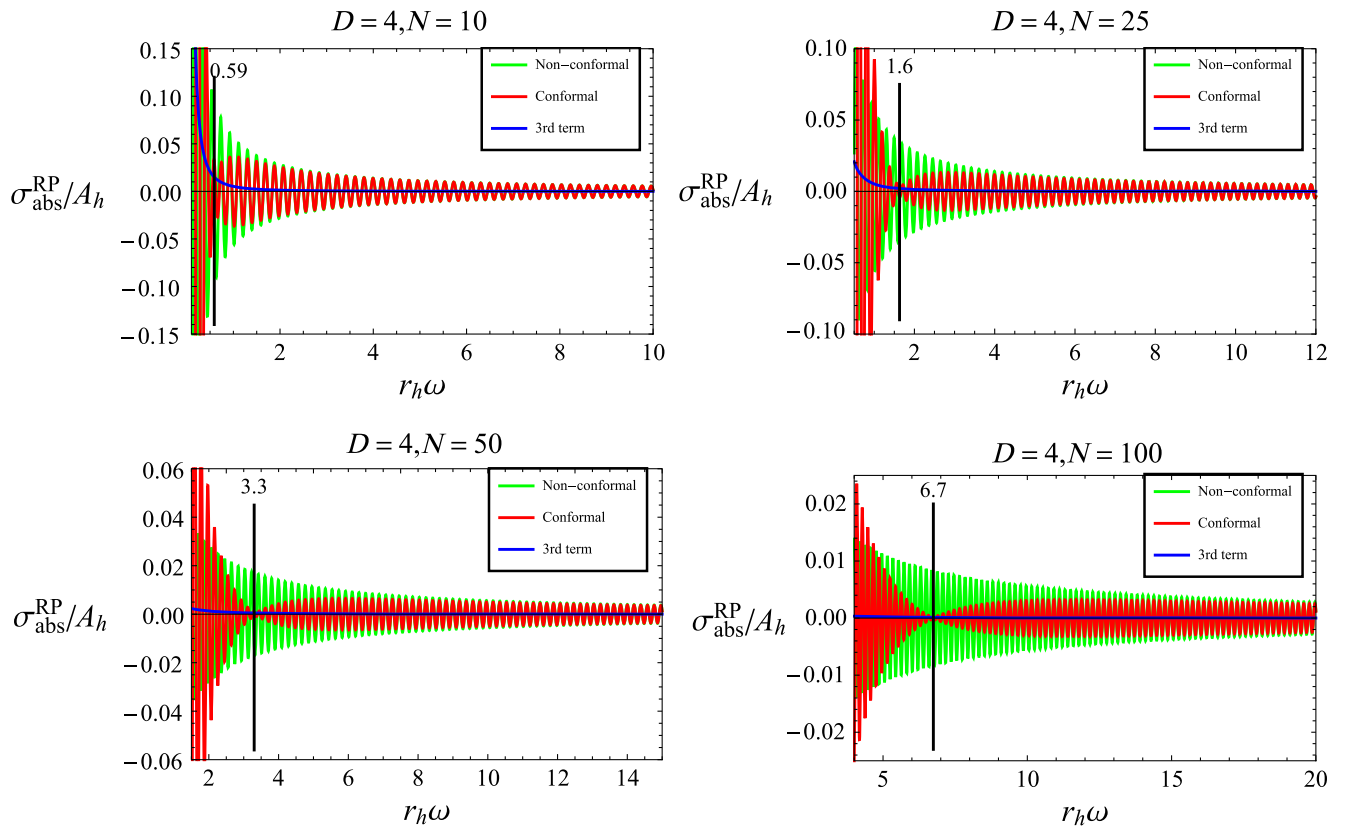


FIG. 3. Comparison between the CRST BHs and ST BHs in the four-dimensional spacetime, where $L = r_c$ and $N = 10, 25, 50, 100$ are set. The red curves stand for the CRST BHs and the green curves for the ST BHs, where the vertical black lines mark the positions of “the minimum amplitude” in the cases of $N = 10, 25, 50, 100$, respectively. The blue curves stand for the upper bound of the third term in Eq. (50). Note that the blue curves are very close to the horizontal axes.

We also find that the behavior of $\sigma_{\text{abs}}^{\text{RP}}(\omega)$ is not sensitive to L . Only when L is ridiculously large, e.g., $L > 2000r_c$ in the four-dimensional CRST BH with $N = 25$, does the non-monotonic behavior vanish according to our numerical calculation. Note that N is the exponent in $S(r)$, while L is a numerator of fraction. It is natural that the influence of N is more prominent than that of L . Furthermore, if the astrophysical data are taken into consideration, the magnitude of L is not likely to be larger than the BH mass in the geometric units [45]. As a result, the nonmonotonic behavior always appears in a physically natural range of L and N .

We end this section with a summary of our results. After some appropriate approximation, we obtain the analytic expressions of $\sigma_{\text{abs}}^{\text{RP}}(\omega)$ for the four-, five-, and six-dimensional CRST BHs. When CRST BHs are reduced to ST BHs, our results agree with the Sinc's [26]. With a specific choice of the scale factor which regularizes the CRST BH spacetimes, the amplitude of $\sigma_{\text{abs}}^{\text{RP}}(\omega)$ of CRST BHs is nonmonotonic, which gives rise to our main conclusion; The CR BHs are substantially different from their nonconformal counterparts in the aspect of ACSs.

VI. CONCLUSION

We analyze the null geodesics of CR BHs and prove the condition, $r_0 \approx r_c$ for $\ell \gg 1$, that is, the location of photon spheres is independent of scale factors in the large- ℓ limit. Then using the third-order WKB approximation together with this condition, we obtain the Regge frequency and the ACS of a massless scalar field absorbed by CR BHs. Our analyses show that the ACSs of CR BHs depend on the scale factor, which can be used to distinguish CR BHs from nonconformal BHs.

To illustrate the distinction, we investigate a specific class of CR BHs, the CRST BHs, and find that there is the nonmonotonic behavior of ACS amplitudes in a wide range of parameter N . This phenomenon manifests the characteristic of CR BHs in the aspect of ACSs.

Significantly, it is possible to use the above mentioned phenomenon to determine observationally the scale factor of CR BHs if the CR BHs exist in our Universe. The scale factor goes to unity asymptotically, so the CR BHs and the nonconformal ones are similar at a large astronomical distance. Nevertheless, we can still distinguish these two kinds of BHs by their absorption spectra. In Ref. [11], the authors concluded that a larger N causes a less violation to the energy condition, which implies that a larger N seems more reasonable and natural in our world. For a larger N , "the minimum amplitude" of $\sigma_{\text{abs}}^{\text{RP}}(\omega)$ appears in the higher-frequency regimes of absorption spectra, which is a more

prominent spectral indication of the scale factor. As for astrophysical experiments, it is technically easier to observe the high-energy rays and particles than the low-energy ones. Therefore, it is feasible to distinguish a CR BH from a nonconformal BH through the observations.

It is also feasible to search for regular BHs in this way. According to the earlier studies [12–16], the ACSs of regular NED BHs do not possess any special spectral characteristics, such as the nonmonotonic behavior. Therefore, the ACSs of NED BHs are indistinguishable from those of singular BHs, such as the Reissner-Nordstrom BH. However, this is not the case for regular CR BHs. The distinction is prominent as we have shown. Therefore, we provide a feasible approach for searching for regular BHs.

Finally, we have an argument about the Hawking radiation of CR BHs. The ACSs are related to the energy flux of Hawking radiation [46–48]. For example, the following formula holds for the four-dimensional Schwarzschild BH,

$$\frac{d^2 E(\omega)}{d\omega dt} \propto \frac{\omega^3 \sigma_{\text{abs}}(\omega)}{\exp(8\pi M\omega) - 1}, \quad (65)$$

which implies that the radiated energy per unit time and unit frequency is proportional to the ACS of four-dimensional Schwarzschild BHs. By integrating Eq. (65) with respect to t and ω , we can obtain the loss of BH energy through the radiation, ΔE . Obviously, ΔE is a function of N and L . This implies that the loss of BH energy does depend on the scale factor $S(r)$ although the Hawking temperature is independent [4–6] of this factor. Such an inference is surprising because it seems that there are unknown properties hidden in the thermodynamics of CR BHs. We believe that the research for the issue will improve our understanding of CR BHs greatly.

ACKNOWLEDGMENTS

The authors would like to thank C. Lan for helpful discussions about the CAM method, analytic S -matrix theory and regular black holes. They would also like to thank the anonymous referee for the helpful comments that improve this work greatly. This work was supported in part by the National Natural Science Foundation of China under Grants No. 11675081 and No. 12175108.

APPENDIX A: THE EXPRESSIONS OF THE TERMS RELATED TO $V_0^{(p)}(\lambda)$

Here we give the asymptotic expansions of the coefficients related to $V_0^{(p)}(\lambda)$ in the limit of $|\lambda| \rightarrow +\infty$.

$$V_0(\lambda) = \frac{f_c}{r_c^2} \lambda^2 + \frac{f_c}{16r_c^2 S_c^2} \{4(D-2)r_c S_c [(D-2)f_c S_c^{(1)} + f_c r_c S_c^{(2)} + 2f_c S_c^{(1)}] + (D-6)(D-2)f_c r_c^2 (S_c^{(1)})^2 + 4S_c^2 [(D-2)Df_c - (D-3)^2]\} + \mathcal{O}\left(\frac{1}{\lambda^2}\right). \quad (A1)$$

$$\begin{aligned}
 [-2V_0^{(2)}(\lambda)]^{1/2} = & \frac{2f_c\eta_c}{r_c^2}\lambda - \frac{1}{16\eta_c r_c^2 S_c^4} \left\{ [8f_c^2 S_c^3 (2(D-2)f_c r_c S_c^{(1)} - S_c((D-3)^2 - 4(D-2)f_c))] \right. \\
 & + 2f_c r_c S_c^2 \left[S_c^2 \left(\frac{4f_c}{r_c} (4(D-2)f_c^{(2)} r_c^2 + 3(D-3)^2) \right. \right. \\
 & + \left. \left. \frac{1}{r_c} 8(D-2)(2d-11)f_c^2 + (D-3)^2 - r_c f_c^{(2)} \right) + 4(D-9)(D-2)f_c^2 r_c (S_c^{(1)})^2 \right. \\
 & + \left. \left. 2(D-2)f_c r_c S_c \left(\frac{2f_c}{r_c} (4(D-2)S_c^{(1)} + 7r_c S_c^{(2)}) + 4f_c^{(2)} r_c S_c^{(1)} \right) \right] \right. \\
 & + \left. f_c^2 S_c (D-2) r_c^3 S_c S_c^{(1)} \left[\frac{2f_c}{r_c} ((5D-46)r_c S_c^{(2)} - 10(D-2)S_c^{(1)}) + (D-10)f_c^{(2)} r_c S_c^{(1)} \right] \right. \\
 & + 4f_c^2 S_c S_c^3 [2(D-2)(22-5D)f_c + (D-6)(D-2)f_c^{(2)} r_c^2 + (D-2) \\
 & + f_c^{(3)} r_c^3 - 3(D-2)^2 + 6(D-2) - 3] + 2f_c^2 S_c (34-5D)(D-2)f_c r_c^3 (S_c^{(1)})^3 \\
 & + 2(D-2)r_c^2 f_c^2 S_c^3 \left[r_c (S_c^{(1)} (2(D-2)f_c^{(2)} + f_c^{(3)} r_c) + 4f_c^{(2)} r_c S_c^{(2)}) \right. \\
 & + \left. \frac{2f_c}{r_c} (r_c (5(D-2)S_c^{(2)} + 6r_c S_c^{(3)}) - 5(D-2)S_c^{(1)}) \right] \\
 & + (D-2)f_c^3 [r_c^3 S_c (S_c^{(1)})^2 ((24-5(D-2))r_c S_c^{(2)} + 4(D-2)S_c^{(1)}) + 3(D-6)r_c^4 (S_c^{(1)})^4 + 12(D-4)S_c^4] \\
 & + (D-2)r_c^2 f_c^3 S_c^2 [r_c S_c^{(1)} ((D-10)r_c S_c^{(3)} - 6(D-2)S_c^{(2)}) + (D-8)r_c^2 (S_c^{(2)})^2 + 4(D-2)(S_c^{(1)})^2] \\
 & + \left. \left. 2(D-2)r_c f_c^3 S_c^3 [r_c ((D-2)r_c S_c^{(3)} - 2(D-2)S_c^{(2)} + r_c^2 S_c^{(4)}) + 2(D-2)S_c^{(1)}] \right\} \frac{1}{\lambda} + \mathcal{O}\left(\frac{1}{\lambda^2}\right). \tag{A2}
 \end{aligned}$$

$$\frac{V_0^{(4)}(\lambda)}{V_0^{(2)}(\lambda)} = -\frac{f_c}{2\eta_c^2 r_c^2} [16f_c^2 - 16r_c^2 f_c f_c^{(2)} + 4r_c^3 f_c f_c^{(3)} (f_c^{(2)})^2 + r_c^4 (4(f_c^{(2)})^2 + f_c f_c^{(4)})] + \mathcal{O}\left(\frac{1}{\lambda^2}\right). \tag{A3}$$

$$\left(\frac{V_0^{(3)}(\lambda)}{V_0^{(2)}(\lambda)} \right)^2 = \frac{r_c^4 f_c^2 (f_c^{(3)})^2}{4\eta_c^4} + \mathcal{O}\left(\frac{1}{\lambda^2}\right). \tag{A4}$$

$$\begin{aligned}
 \frac{[V_0^{(3)}(\lambda)]^2 V_0^{(4)}(\lambda)}{[V_0^{(2)}(\lambda)]^3} = & -\frac{r_c^2 f_c^3 (f_c^{(3)})^2}{8\eta_c^6} [16f_c^2 - 16r_c^2 f_c f_c^{(2)} + 4r_c^3 f_c f_c^{(3)} (f_c^{(2)})^2 \\
 & + r_c^4 (4(f_c^{(2)})^2 + f_c f_c^{(4)})] + \mathcal{O}\left(\frac{1}{\lambda^2}\right). \tag{A5}
 \end{aligned}$$

$$\frac{V_0^{(3)}(\lambda) V_0^{(5)}(\lambda)}{[V_0^{(2)}(\lambda)]^2} = \frac{r_c^2 f_c^3 f_c^{(3)}}{4\eta_c^4} [-10f_c f_c^{(3)} + 10r_c f_c f_c^{(4)} + r_c^2 (15f_c^{(2)} f_c^{(3)} + f_c f_c^{(5)})] + \mathcal{O}\left(\frac{1}{\lambda^2}\right). \tag{A6}$$

$$\begin{aligned}
 \frac{V_0^{(6)}(\lambda)}{V_0^{(2)}(\lambda)} = & -\frac{f_c^2}{2\eta_c^2 r_c^4} [-272f_c^3 + 408r_c^2 f_c^2 f_c^{(2)} - 88r_c^3 f_c^2 f_c^{(3)} (f_c^{(2)})^2 \\
 & + r_c^4 f_c (38f_c f_c^{(4)} - 204(f_c^{(2)})^2) + r_c^5 f_c (104f_c^{(2)} f_c^{(3)} + 18f_c f_c^{(5)}) (f_c^{(2)})^2 \\
 & + r_c^6 (34(f_c^{(2)})^3 + 15f_c (f_c^{(3)})^2 + 26f_c f_c^{(2)} f_c^{(4)} + f_c^2 f_c^{(6)})] + \mathcal{O}\left(\frac{1}{\lambda^2}\right). \tag{A7}
 \end{aligned}$$

The expansions are kept to $\mathcal{O}(1/\lambda^2)$ in the limit of $|\lambda| \rightarrow +\infty$, where the scale factor only appears in $V_0(\lambda)$ and $[-2V_0^{(2)}(\lambda)]^{1/2}$; see Eqs. (A1) and (A2).

APPENDIX B: THE EXPRESSIONS OF a_n AND b_n

We find that the terms proportional to $[\alpha(n)]^2$ do not include S_c or $S_c^{(p)}$ in a_n and b_n .

$$\begin{aligned}
 a_n = & -\frac{1}{1152\eta_c^4} \left\{ -72f_c^2(4f_c - 2r_c^2f_c^{(2)}) - 7r_c^6f_c(f_c^{(3)})^2 - 36r_c^3f_c f_c^{(3)}(2f_c - r_c^2f_c^{(2)}) \right. \\
 & - 18(4f_c - 2r_c^2f_c^{(2)})[(D-3)^2(4f_c - 2r_c^2f_c^{(2)}) + r_c^4(f_c^{(2)})^2] \\
 & + \frac{9f_c}{2S_c^2}(4f_c - 2r_c^2f_c^{(2)})[(D-2)(4f_c - 2r_c^2f_c^{(2)}) + 16r_c^2S_c^2f_c^{(2)} - r_c^4S_c^2f_c^{(4)} \\
 & \left. + 4Dr_cS_cS_c^{(1)} + 4r_c^2S_cS_c^{(2)} + (D-6)r_c^2(S_c^{(1)})^2 + 4DS_c^2] \right\} \\
 & + [\alpha(n)]^2 \frac{r_c^3f_c}{96\eta_c^4} \{24f_c f_c^{(3)} + 6r_c f_c f_c^{(4)} - 12r_c^2 f_c^{(2)} f_c^{(3)} + r_c^3[5(f_c^{(3)})^2 - 3f_c^{(2)} f_c^{(4)}]\}. \tag{B1}
 \end{aligned}$$

$$\begin{aligned}
 b_n = & \frac{1}{442368\eta_c^{10}} \left\{ 385r_c^{12}f_c^2(f_c^{(3)})^4 + 459r_c^6f_c(f_c^{(3)})^2(4f_c - 2f_c^{(2)}r_c^2) \right. \\
 & \times [4r_c^3f_c f_c^{(3)} + r_c^4f_c f_c^{(4)} - 16r_c^2f_c f_c^{(2)} + 16f_c^2 + 4r_c^4(f_c^{(2)})^2] \\
 & + 201(2f_c - r_c^2f_c^{(2)})^2[4r_c^3f_c f_c^{(3)} + r_c^4f_c f_c^{(4)} - 16r_c^2f_c f_c^{(2)} + 16f_c^2 + 4r_c^4(f_c^{(2)})^2]^2 \\
 & + 456r_c^6f_c f_c^{(3)}(2f_c - r_c^2f_c^{(2)})^2[10r_c f_c f_c^{(4)} + r_c^2f_c f_c^{(5)} - 10f_c f_c^{(3)} + 15r_c^2f_c^{(2)} f_c^{(3)}] \\
 & + 120(2f_c - f_c^{(2)}r_c^2)^3[104r_c^5f_c f_c^{(2)} f_c^{(3)} + 26r_c^6f_c f_c^{(2)} f_c^{(4)} - 204r_c^4f_c(f_c^{(2)})^2 + 15r_c^6f_c(f_c^{(3)})^2 \\
 & - 272f_c^3 + 34r_c^6(f_c^{(2)})^3 + 408r_c^2f_c^2f_c^{(2)} - 88r_c^3f_c^2f_c^{(3)} + 38r_c^4f_c^2f_c^{(4)} + 18r_c^5f_c^2f_c^{(5)} + r_c^6f_c^2f_c^{(6)}] \\
 & - \frac{864}{S_c^4}(2f_c - f_c^{(2)}r_c^2)^4[-2(D-3)^2r_c^2S_c^4f_c^{(2)} + f_cS_c^2((D-10)(D-2)r_c^4(S_c^{(1)}f_c^{(2)})^2 \\
 & + 4S_c^2((D-3)^2 + (D^2-4)r_c^2f_c^{(2)} + (D-2)r_c^3f_c^{(3)}) + 4(D-2)r_c^3S_c f_c^{(2)}((D+2)S_c^{(1)} + 4r_cS_c^{(2)}f_c^{(2)} + r_cS_c^{(1)}f_c^{(3)})) \\
 & + (D-2)f_c^2((34-5D)r_c^4S_c(S_c^{(1)})^2S_c^{(2)} - 6(D-10)r_c^3S_c(S_c^{(1)})^3 + 3(D-6)r_c^4(S_c^{(1)})^4 + 4(D-4)S_c^4 \\
 & + (D-2)r_c^2S_c^2f_c^2((D-10)r_c^2S_c^{(1)}S_c^{(3)} + 4(D-20)r_cS_c^{(1)}S_c^{(2)} + (D-8)r_c^2(S_c^{(2)})^2 - 8(D+5)(S_c^{(1)})^2) \\
 & \left. + 2(D-2)r_cS_c^3f_c^2(8(D-1)S_c^{(1)} + 4(2D+3)r_cS_c^{(2)} + (D+10)r_c^2S_c^{(3)} + r_c^3S_c^{(4)})] \right\} \\
 & + [\alpha(n)]^2 \frac{r_c^3f_c}{110592\eta_c^{10}} \{9216f_c^4f_c^{(3)} + 13824r_c f_c^4f_c^{(4)} + 3456r_c^2f_c^3[-2f_c^{(2)}f_c^{(3)} + f_c f_c^{(5)}] \\
 & + 192r_c^3f_c^3[72(f_c^{(3)})^2 - 99f_c^{(2)}f_c^{(4)} + f_c f_c^{(6)}] - 288r_c^4f_c^2[12(f_c^{(2)})^2f_c^{(3)} - 29f_c f_c^{(3)}f_c^{(4)} + 18f_c f_c^{(2)}f_c^{(5)}] \\
 & + 12r_c^5f_c^2[648(f_c^{(2)})^2f_c^{(4)} + 17f_c f_c^{(4)}^2 + 56f_c f_c^{(3)}f_c^{(5)} - 1032f_c^{(2)}(f_c^{(3)})^2 - 24f_c f_c^{(2)}f_c^{(6)}] \\
 & + 144r_c^6f_c[28(f_c^{(2)})^3f_c^{(3)} + 25f_c(f_c^{(3)})^3 - 58f_c f_c^{(2)}f_c^{(3)}f_c^{(4)} + 18f_c(f_c^{(2)})^2f_c^{(5)}] \\
 & + 12r_c^7f_c[-36(f_c^{(2)})^3f_c^{(4)} + 75f_c(f_c^{(3)})^2f_c^{(4)} - 17f_c f_c^{(2)}(f_c^{(4)})^2 - 56f_c f_c^{(2)}f_c^{(3)}f_c^{(5)} \\
 & + 168(f_c^{(2)})^2(f_c^{(3)})^2 + 12f_c(f_c^{(2)})^2f_c^{(6)}] - 72r_c^8f_c^{(2)}[12(f_c^{(2)})^3f_c^{(3)} + 25f_c(f_c^{(3)})^3 - 29f_c f_c^{(2)}f_c^{(3)}f_c^{(4)} + 6f_c(f_c^{(2)})^2f_c^{(5)}] \\
 & + r_c^9[235f_c(f_c^{(3)})^4 - 216(f_c^{(2)})^4f_c^{(4)} - 450f_c f_c^{(2)}(f_c^{(3)})^2f_c^{(4)} + 51f_c(f_c^{(2)})^2(f_c^{(4)})^2 \\
 & \left. + 168f_c(f_c^{(2)})^2f_c^{(3)}f_c^{(5)} + 360(f_c^{(2)})^3(f_c^{(3)})^2 - 24f_c(f_c^{(2)})^3f_c^{(6)}]\}. \tag{B2}
 \end{aligned}$$

- [1] H. Weyl, Reine infinitesimalgeometrie, *Math. Z.* **2**, 384 (1918).
- [2] M.P. Dabrowski, J. Garecki, and D.B. Blaschke, Conformal transformations and the conformal invariance in gravitation, *Ann. Phys. (Berlin)* **18**, 13 (2009).
- [3] Y. Fujii and K.I. Maeda, *The Scalar-Tensor Theory of Gravitation* (Cambridge University Press, Cambridge, England, 2003).
- [4] L. Modesto and L. Rachwal, Finite conformal quantum gravity and nonsingular spacetimes, [arXiv:1605.04173](https://arxiv.org/abs/1605.04173).
- [5] C. Bambi, L. Modesto, and L. Rachwal, Spacetimes completeness of non-singular black holes in conformal gravity, *J. Cosmol. Astropart. Phys.* **05** (2017) 003.
- [6] Y. Li and Y.-G. Miao, Distinct thermodynamic and dynamic effects produced by scale factors in conformally related Einstein-power-Yang-Mills black holes, *Phys. Rev. D* **104**, 024002 (2021).
- [7] B. Toshmatov, C. Bambi, B. Ahmedov, Z. Stuchlík, and J. Schee, Scalar perturbations of nonsingular nonrotating black holes in conformal gravity, *Phys. Rev. D* **96**, 064028 (2017).
- [8] C. Y. Chen and P. Chen, Gravitational perturbations of non-singular black holes in conformal gravity, *Phys. Rev. D* **99**, 104003 (2019).
- [9] C. Bambi, L. Modesto, S. Porey, and L. Rachwal, Black hole evaporation in conformal gravity, *J. Cosmol. Astropart. Phys.* **09** (2017) 033.
- [10] C. Bambi, L. Modesto, S. Porey, and L. Rachwal, Formation and evaporation of an electrically charged black hole in conformal gravity, *Eur. Phys. J. C* **78**, 116 (2018).
- [11] B. Toshmatov, C. Bambi, B. Ahmedov, A. Abdujabbarov, and Z. Stuchlík, Energy conditions of non-singular black hole spacetimes in conformal gravity, *Eur. Phys. J. C* **77**, 542 (2017).
- [12] C. F. B. Macedo and L. C. B. Crispino, Absorption of planar massless scalar waves by Bardeen regular black holes, *Phys. Rev. D* **90**, 064001 (2014).
- [13] C. F. B. Macedo, E. S. de Oliveira, and L. C. B. Crispino, Scattering by regular black holes: Planar massless scalar waves impinging upon a bardeen black hole, *Phys. Rev. D* **92**, 024012 (2015).
- [14] P.A. Sanchez and N. Bretón, and S.E.P. Bergliaffa, Scattering and absorption of massless scalar waves by Born-Infeld black holes, *Ann. Phys. (Amsterdam)* **393**, 107 (2018).
- [15] S. Fernando, Bardeen-de Sitter black holes, *Int. J. Mod. Phys. D* **26**, 1750071 (2017).
- [16] M.A.A. Paula, L.C.S. Leite, and L.C.B. Crispino, Electrically charged black holes in linear and nonlinear electrodynamics: Geodesic analysis and scalar absorption, *Phys. Rev. D* **102**, 104033 (2020).
- [17] G.N. Watson, The transmission of electric waves round the Earth, *Proc. R. Soc. A* **95**, 546 (1919).
- [18] R.G. Newton, *Scattering Theory of Waves and Particles* (Springer-Verlag, New York, 1982).
- [19] H.M. Nussenzveig, *Diffraction Effects in Semi-classical Scattering* (Cambridge University Press, Cambridge, England, 1992).
- [20] S. Chandrasekhar and V. Ferrari, On the nonradial oscillations of a star. 4: An application of the theory of Regge poles, *Proc. R. Soc. A* **437**, 133 (1992).
- [21] N. Andersson and K. E. Thylwe, Complex angular momentum approach to black hole scattering, *Classical Quant. Grav.* **11**, 2991 (1994).
- [22] N. Andersson, Complex angular momenta and the black hole glory, *Classical Quant. Grav.* **11**, 3003 (1994).
- [23] Y. Decanini, A. Folacci, and B. Jensen, Complex angular momentum in black hole physics and the quasinormal modes, *Phys. Rev. D* **67**, 124017 (2003).
- [24] Y. Decanini and A. Folacci, Regge poles of the Schwarzschild black hole: A WKB approach, *Phys. Rev. D* **81**, 024031 (2010).
- [25] Y. Decanini, A. Folacci, and B. Raffaelli, Unstable circular null geodesics of static spherically symmetric black holes, Regge poles and quasinormal frequencies, *Phys. Rev. D* **81**, 104039 (2010).
- [26] Y. Decanini, G. Esposito-Farese, and A. Folacci, Universality of high-energy absorption cross sections for black holes, *Phys. Rev. D* **83**, 044032 (2011).
- [27] Y. Decanini, A. Folacci, and B. Raffaelli, Fine structure of high-energy absorption cross sections for black holes, *Classical Quant. Grav.* **28**, 175021 (2011).
- [28] Y. Decanini, A. Folacci, and B. Raffaelli, Resonance and absorption spectra of the Schwarzschild black hole for massive scalar perturbations: A complex angular momentum analysis, *Phys. Rev. D* **84**, 084035 (2011).
- [29] A. Folacci and A. Tamar, Quasinormal mode frequencies of Kerr black holes from Regge trajectories, [arXiv:2103.01258](https://arxiv.org/abs/2103.01258).
- [30] S. R. Dolan and A. C. Ottewill, On an expansion method for black hole quasinormal modes and Regge poles, *Classical Quant. Grav.* **26**, 225003 (2009).
- [31] E. Berti, V. Cardoso, and A. O. Starinets, Quasinormal modes of black holes and black branes, *Classical Quant. Grav.* **26**, 163001 (2009).
- [32] K. D. Kokkotas and B. G. Schmidt, Quasi-normal modes of stars and black holes, *Living Rev. Relativity* **2**, 2 (1999).
- [33] H. P. Nollert, The characteristic ‘sound’ 788 of black holes and neutron stars, *Classical Quant. Grav.* **16**, R159 (1999).
- [34] R. A. Konoplya and A. Zhidenko, Quasinormal modes of black holes: From astrophysics to string theory, *Rev. Mod. Phys.* **83**, 793 (2011).
- [35] S. Chandrasekhar, *The Mathematical Theory of Black Holes* (Oxford University Press, New York, 1983).
- [36] V. Cardoso, A. S. Miranda, E. Berti, H. Witek, and V. T. Zanchin, Geodesic stability, Lyapunov exponents and quasinormal modes, *Phys. Rev. D* **79**, 064016 (2009).
- [37] J. J. Sakurai and J. Napolitano, *Modern Quantum Mechanics* (Addison-Wesley, San Francisco, 2011).
- [38] B. F. Schutz and C. M. Will, Black hole normal modes: A semianalytic approach, *Astrophys. J. Lett.* **291**, L33 (1985).
- [39] S. Iyer and C. M. Will, Black hole normal modes: A WKB approach. I. Foundations and application of a higher-order WKB analysis of potential-barrier scattering, *Phys. Rev. D* **35**, 3621 (1987).
- [40] R. A. Konoplya, Quasinormal behavior of the D-dimensional Schwarzschild black hole and the higher order WKB approach, *Phys. Rev. D* **68**, 024018 (2003).

- [41] R. A. Konoplya, A. Zhidenko, and A. F. Zinhailo, Higher order WKB formula for quasinormal modes and grey-body factors: Recipes for quick and accurate calculations, *Classical Quant. Grav.* **36**, 155002 (2019).
- [42] J. Matyjasek and M. Telecka, Quasinormal modes of black holes. II. Padé summation of the higher-order WKB terms, *Phys. Rev. D* **100**, 124006 (2019).
- [43] C. M. Harris and P. Kanti, Hawking radiation from a (4+n)-dimensional black hole: Exact results for the Schwarzschild phase, *J. High Energy Phys.* **10** (2003) 014.
- [44] S. S. Gubser, Can the effective string see higher partial waves?, *Phys. Rev. D* **56**, 4984 (1997).
- [45] C. Bambi, Z. Cao, and L. Modesto, Testing conformal gravity with the supermassive black hole in 1H0707-495, *Phys. Rev. D* **98**, 024007 (2018).
- [46] P. Kanti and E. Winstanley, Hawking radiation from higher-dimensional black holes, *Fundam. Theor. Phys.* **178**, 229 (2015).
- [47] D. N. Page, Particle emission rates from a black hole: Massless particles from an uncharged, nonrotating hole, *Phys. Rev. D* **13**, 198 (1976).
- [48] D. N. Page, Particle emission rates from a black hole. II. Massless particles from a rotating hole, *Phys. Rev. D* **14**, 3260 (1976).